Gooley, P. R., Caffrey, M. S., Cusanovich, M. A., & MacKenzie, N. E. (1991a) *Eur. J. Biochem. 196*, 653–661.
Gooley, P. R., Zhao, D., & MacKenzie, N. E. (1991b) *J. Biomol. Nucl. Magn. Reson. 1*, 145–154.
Hvidt, A., & Nielsen, S. O. (1966) *Adv. Protein Chem. 21*, 287–386.
Jandu, S. K., Ray, S., Brooks, L., & Leatherbarrow, R. J. (1990) *Biochemistry 29*, 6264–6269.
Kassner, R. J. (1972) *Proc. Natl. Acad. Sci. U.S.A. 69*, 2263–2267.
Koshy, T. I., Luntz, T. L., Schejter, A., & Margoliash, E. (1990) *Proc. Natl. Acad. Sci. U.S.A. 87*, 8697–8701.
Kuwajima, K., & Baldwin, R. L. (1983) *J. Mol. Biol. 169*, 299–323.
Linse, S., Teleman, O., & Drankenberg, T. (1990) *Biochemistry 29*, 5925–5934.
Loll, P. J., & Lattman, E. E. (1990) *Biochemistry 29*, 6866–6873.
Louie, G. V., & Brayer, G. D. (1990) *J. Mol. Biol. 214*, 527–555.
Luntz, T. L., Schejter, A., Garber, E. A. E., & Margoliash, E. (1989) *Proc. Natl. Acad. Sci. U.S.A. 86*, 3524–3528.
Molday, R. S., Englander, S. W., & Kallen, R. G. (1972) *Biochemistry 11*, 150–158.
Pace, C. N., Laurents, D. V., & Thomson, J. A. (1990) *Biochemistry 29*, 2564–2572.
Pardi, A., Wagner, G., & Wüthrich, K. (1983) *Eur. J. Biochem. 137*, 445–454.
Roder, H., Wagner, G., & Wüthrich, K. (1985) *Biochemistry 24*, 7396–7407.
Takano, T., & Dickerson, R. E. (1981a) *J. Mol. Biol. 153*, 79–94.
Takano, T., & Dickerson, R. E. (1981b) *J. Mol. Biol. 153*, 95–115.
Wagner, G. (1983) *Q. Rev. Biophys. 16*, 1–57.
Wagner, G., & Wüthrich, K. (1982) *J. Mol. Biol. 160*, 343–361.
Wagner, G., Stassinopoulou, G., & Wüthrich, K. (1984) *Eur. J. Biochem. 145*, 431–436.
Wand, A. J., Roder, H., & Englander, S. W. (1986) *Biochemistry 25*, 1107–1114.
Wüthrich, K., Strop, P., Ebina, S., & Williamson, M. P. (1984) *Biochem. Biophys. Res. Commun. 122*, 1174–1178.

Experimental and Computational Infrared CD Studies of Prototypical Peptide Conformations†

Sheryl S. Birke, Ismailu Agbaje, and Max Diem*

Departments of Chemistry and Biochemistry, Hunter College, The City University of New York, 695 Park Avenue, New York, New York 10021

Received May 15, 1991; Revised Manuscript Received October 8, 1991

ABSTRACT: The infrared vibrational circular dichroism (VCD) spectral features of prototypical peptide secondary structures were reported previously by Yasui and Keiderling [Yasui, S. C., & Keiderling, T. A. (1986) *Biopolymers 25*, 5]. These results demonstrated that the "random coil" peptide conformation exhibits VCD signals which are approximately mirror-image features of those exhibited by α-helical conformers. We report here a comparison of observed VCD spectra with those computed for several secondary structures, using the extended coupled oscillator formalism employed previously to compute VCD spectra of model DNA [Zhong et al. (1990) *Biochemistry 29*, 7485]. These studies suggest that the so-called random-coil peptide conformation has distinct short-range order and appears to be a left-handed, helical structure.

The peptide backbone exists in a number of distinct and well-known conformations, determined by the value of the ϕ and ψ angles (Schulz & Schirmer, 1979). Among the most common of these conformations is the right-handed α-helix, which shows distinct CD features described by Holzwarth and Doty (1965) and Greenfield and Fasman (1969). The aforementioned angles ϕ and ψ associated with the right-handed α-helix fall into a broad minimum energy region in the Ramachandran plot for peptides, centered about −55°, −55°.

Many α-helical model peptides can be induced to undergo a phase transition by varying the acidity or the ionic strength of the solvent. Poly(L-lysine), for example, exists in an α-helical form at a pH above 10.6. When the medium is acidified, a distinct phase transition to another conformer occurs, which exhibits CD spectra which are smaller in amplitude than those of the α-helix, and are inverted in sign. This conformation has been referred to as the "random coil" form.

The first conformation-dependent VCD spectra of polyamino acids were reported by Yasui and Keiderling (1986a,b) for poly(L-tyrosine) (PLT) in DMSO, and nearly simultaneously by Keiderling's and Nafie's groups for poly(L-lysine) (PLL) in aqueous solution (Yasui & Keiderling, 1986a,b; Paterlini et al., 1986). This last study showed unequivocally that a true random conformation, obtained by denaturation of PLL, shows minimal VCD signals in the amide I′ region. On the basis of the sign pattern of the observed VCD couplet, this publication also suggested that the "random coil" conformation is actually a left-handed helical structure. VCD,

† This research was supported by the National Institute of General Medical Sciences (GM 28619). The construction of the VCD instruments was supported by grants from the NSF (CHE 86-07934), by several CUNY faculty research awards, and by Instruments, SA, Metuchen, NJ. The molecular graphics workstation was purchased through an RCMI grant (RR 03037) to the Division of Science and Mathematics at Hunter College.

* Address correspondence to this author at the Department of Chemistry, Hunter College of The City University of New York.

0006-2960/92/0431-450$03.00/0

which has been reviewed a number of times recently [see, for example, Keiderling (1990)], is an ideal tool to study the conformation of polypeptides in solution phase. Like in CD, most of the observed signals in polypeptides are due to the dipolar coupling of the transition moments localized on the peptide linkages. Unlike CD, where there are at least two overlapping transitions ($\pi^* \leftarrow \pi$ and $\pi^* \leftarrow$ n) which form the exciton manifold in the 180–230-nm region, the wavelength range in VCD can be selected such that only one transition contributes. Furthermore, the bandwidth of a typical vibrational band is about the same as the exciton splitting. Thus, relatively sharp and distinct VCD spectra are obtained.

Vibrational transition moments are smaller than the electronic counterparts in the amide moiety. Thus, the coupling in VCD extends over shorter distances than in electronic CD, and, therefore, VCD is sensitive to structural order which extends over shorter distances than that responsible for the electronic CD. Finally, the direction of the dipole transition moment is less ambiguous in VCD than in CD, and is nearly parallel to the direction of the C–O bond for the amide I vibration. This simplifies the computational procedures, which can be adapted readily from procedures derived for electronic exciton interactions (Tinoco, 1963).

Thus, VCD is a powerful method to quantitatively determine the conformation of peptides in solution. We have previously solved the solution structure of a small peptide, (L-Ala)$_3$, in aqueous solution via the vibrational exciton approach (Lee et al., 1989). In this paper, we present computational results for the α-helical conformation to establish that the "extended coupled oscillator" (ECO) formalism, which we have applied successfully to the computation of DNA VCD spectra, also is applicable to model peptides. Original VCD intensity calculations for helical polymers were carried out before experimental data were available (Deutsche & Moscowitz, 1968, 1970; Snir et al., 1975; Schellman, 1974). Some aspects of experimental and prior theoretical results were discussed by Lipp and Nafie (1985). The present paper represents the first attempt to directly compare observed and computed VCD data for the α-helical conformation, and evaluate the validity of the model chosen.

Finally, we present calculated VCD spectral results for some known left-handed structures and compare these results to the experimental data for the "random coil" conformation. These studies suggest that this "random coil" conformer is either one of two left-handed helices for which the calculated VCD spectra are virtually indistinguishable. One of these structures falls into the range of left-handed α-helicity, with conformational angles $\phi = 60°$ and $\psi = 30°$, and with about three residues per turn. The other possible structure lies in the broad energy minimum centered around $\phi = -120°$ and $\psi = 120°$. In this region, the pleated sheet structures and various known left-handed helical structures (with $\phi \approx -100°$ and ψ between 100° and 130°) occur. Both these structures reproduce the VCD spectra observed for the so-called random-coil conformation nearly equally well.

Materials and Methods

All infrared absorption and VCD spectra reported here were collected on a dispersive VCD instrument, optimized in the 6-μm region, but otherwise very similar to a mid-IR VCD instrument described earlier (Diem et al., 1988). The VCD spectra reported here were acquired at a spectral resolution of about 5 cm^{-1}.

Commercial samples (Sigma Chemical Corp) of poly(L-tyrosine) (PLT) with chain lengths between 50 and 500 were used after freeze-drying to remove indeterminate amounts of water contaminating the samples. DMSO was distilled from CaH_2 to destroy water. Water in either the solvent or the sample mostly perturbs the infrared absorption spectra at 1620 cm^{-1} and distorts the intensities in the amide I region. However, water does not seem to affect the secondary structures observed, since the VCD spectra are virtually independent of the presence of trace amounts of water.

Sample concentration was between 15 and 50 mg of peptide/mL of solution. The exact conditions are reported in the figure captions. All samples were contained in cells consisting of 32-mm-diameter CaF_2 windows with Teflon spacers of appropriate thickness, between 15 and 50 μm. The total sample volume required is between 15 and 30 μL. All results are reported in units of ϵ (liters per mole per centimeter) per residue.

For acidic solutions, DMSO was acidified by adding trifluoroacetic acid (TFA) or trichloroacetic acid (TCA). The TFA used was not completely dry; thus, the IR absorption spectra of samples containing this acid show various water peaks in the 1600–1700 cm^{-1} region. These acids were selected over dichloroacetic acid (DCA) used by Keiderling in his original studies (Yasui & Keiderling, 1986a), since we also investigated the amide III region, where DCA is not transparent. The amide III results will be reported at a later date.

Computational Procedures

Infrared absorption and VCD intensity calculations were carried out via the extended coupled oscillator (ECO) formalism, which is based on Tinoco's exciton description of the rotatory power of polymers (Tinoco, 1963). In this formalism, the rotational strengths for each of the k exciton components of an n-mer of coupled transitions can be written as (Gulotta et al., 1989)

$$R_k = -(\pi\tilde{\nu}_0/c)\sum_{i=1}^{n}\sum_{j>i}^{n}\mathbf{c}_{ik}\mathbf{c}_{jk}[\mathbf{T}_{ij}\cdot\boldsymbol{\mu}_i \times \boldsymbol{\mu}_j] \quad (1)$$

Here, $\boldsymbol{\mu}_i$ and $\boldsymbol{\mu}_j$ are the interacting dipole moments, separated by vector $\mathbf{T}_{ij}$, $\tilde{\nu}_0$ is the frequency of the uncoupled transition, and c the velocity of light. The $\mathbf{c}_{ij}$ are the eigenvector components of the dipole–dipole interaction matrix $\mathbf{V}_{ij}$:

$$\mathbf{V}_{ij} = \frac{\boldsymbol{\mu}_i\cdot\boldsymbol{\mu}_j}{|\mathbf{T}_{ij}|^3} - \frac{3(\boldsymbol{\mu}_i\cdot\mathbf{T}_{ij})(\boldsymbol{\mu}_j\cdot\mathbf{T}_{ij})}{|\mathbf{T}_{ij}|^5} \quad (2)$$

Each of the terms in the summation in eq 1 is equivalent to a coupled oscillator expression for a simple coupled dimer. The summation is over all pairwise interactions, weighted by the eigenvector coefficients. Inclusion of all coupling interactions is particular important in peptide helices, where the coupling energy between carbonyl group i and i+3 is still relatively large (Snir et al., 1975).

The ECO expression in eq 1 above formally appears similar to the fixed partial charge equation derived by Schellman (1973). However, eq 1 is accurate within the exciton formalism and relies only on observable quantities, such as the dipole transition moment and geometric parameters.

The infrared absorption intensities can be obtained from the dipole strengths, D, defined by

$$D_k = \sum_{i=1}^{n}\mathbf{c}_{ik}^2\boldsymbol{\mu}_i^2 + \sum_{i=1}^{n}\sum_{j>i}^{n}\mathbf{c}_{ik}\mathbf{c}_{jk}(\boldsymbol{\mu}_i\cdot\boldsymbol{\mu}_j) \quad (3)$$

The computations are carried out as follows. Structures for various peptide conformations were generated using the program MacroModel (Still, 1989), running on a MicroVAX/Evans & Sutherland PS 390 Graphics workstation. Macro-

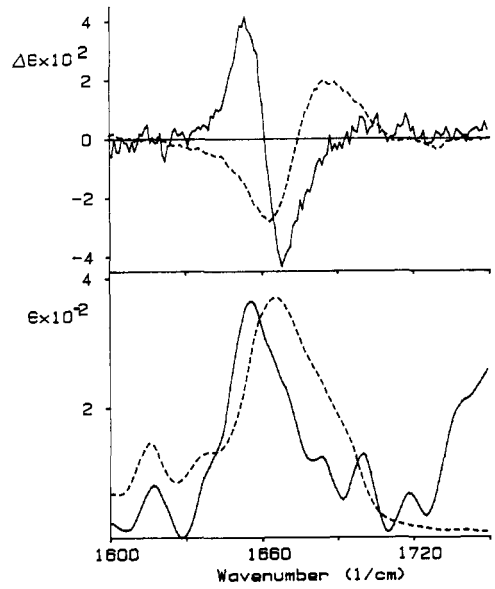

FIGURE 1: Observed infrared VCD (top) and absorption spectra (bottom) of poly(L-tyrosine) in (solid trace) DMSO/TFA (20% by volume). Sample concentration, 42 mg/mL; path length, 15 μm. (Dashed trace) DMSO. Sample concentration, 23 mg/mL; path length, 15 μm.

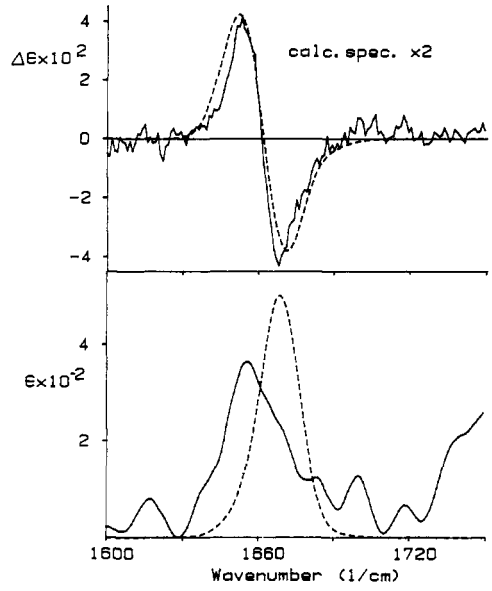

FIGURE 2: Observed (solid traces) and computed (dashed traces) spectra of α-helical poly(L-tyrosine). Experimental conditions: same as in Figure 1. Computational conditions: octamer, $\phi = -52°$, $\psi = -53°$.

Model permits the creation of peptide structures using predetermined conformational angles for right- and left-handed α-helices, as well as for a number of other common structures. Alternatively, the ϕ and ψ angles may be input manually to create less common structures. Amino acid sequence may be specified; however, in this study, homooligopeptides with chain lengths of between 8 and 30 residues were specified. No energy minimization of the structures was performed, since it is important for the following VCD calculations that the structures are the ones actually specified via the input parameters. Originally, tyrosine residues were used to construct the atomic coordinates. However, since no energy minimization was performed, alanine residues were used for the final calculations, because only the backbone structure was desired, which is virtually identical for $(L\text{-Ala})_8$ and $(L\text{-Tyr})_8$. Both models gave identical results in the VCD exciton calculations, because the nature of the side chain has no effect on the VCD exciton calculations.

The Cartesian coordinates of all atoms of the peptides were fed into the ECO program, written in our laboratory, which selects the carbonyl C and O atoms, and attaches transition dipole moments along the C=O bond. The dipole transition moment for an amide I vibration was taken to be $\mu = 0.29$ $D = 0.29 \times 10^{-18}$ esu cm, in agreement with the work by Snir et al. (1975) and our own previous peptide VCD data.

The rotational and dipole strengths R_k and D_k calculated from the ECO program were converted to spectra by overlaying Gaussian, Lorentzian, or mixed band shapes. In the results reported here, 100% Gaussian band shapes with a half-width (at half-heights) of 9 cm^{-1} were used. The resulting spectra are converted to ϵ units and normalized with respect to the number of residues in the computed structures.

Results and Discussion

Figure 1 shows the infrared absorption and VCD spectra of poly(L-tyrosine) in the amide I region, in both the α-helical and the "random coil" conformer. These spectral results had been reported previously (Yasui & Keiderling, 1986a,b), and similar features, with similar $\Delta\epsilon/\epsilon$ values, are observed for other polyamino acids as well. Thus, one can conclude that these features are due to the secondary structure of the peptide under investigation, and are independent of the nature of the side group.

The inversion of the VCD features between the helical and the "random coil" structures is readily apparent. The magnitude of the "random coil" VCD, which is only slightly smaller than that of the α-helical form, suggests that the "random coil" has short-range order similar to that found in the α-helix, but presumably with opposite handedness. In a number of previous investigations [see, for example, Sengupta and Krimm (1987)], the possibility for a relatively ordered state of this "random coil" conformation was proposed. We have calculated the expected VCD for some of these proposed conformations, and have compared it to the observed VCD of the "random coil".

First, the computational procedures were calibrated by reproducing the spectra observed for the α-helical conformation. The structural parameters of this conformation are well established. However, the question arises whether or not the conformation observed at concentrations typically used for VCD studies is the same as the one observed in CD studies (Wen & Woody, 1975). We have varied the concentration and have not observed any changes in the VCD features when the acid (TFA) concentration is constant. However, at low acid concentrations, the observed VCD spectra depend on the sample concentrations: at low PLT concentration, the random coil is observed, whereas high sample concentrations favor a transition to the α-helical form. This behavior will be discussed in more detail in a later publication. Nevertheless, at the concentration shown, PLT exhibits VCD features similar to those observed for other α-helical peptides, and we are certain that we are dealing with an α-helical peptide.

Using carbonyl coordinates created by MacroModel and the computational procedures discussed above, we obtained calculated spectra for the α-helical form shown in Figure 2. These calculations use the correct coordinates of the carbonyl groups, and dipole transition directions along the C=O bond direction. Our computational results contain both the helical contributions as well as the Moffit terms (Schellman & Becktel, 1983).

The results agree reasonably well with the previous calculations by Schellman and co-workers (Snir et al., 1975).

However, our computations are smaller by a factor of 5 than those reported previously, and thus are closer to the experimental values. However, the calculations by Schellman's group used a different approach within the exciton formalism than our calculations. Nevertheless, it is gratifying to see that many of the features agree very well between the two models: the interaction energies between peptide linkages i, $i+1$, $i+2$, and $i+3$ used by Schellman, based on the empirical data by Miyazawa and Blout (1961), are identical in sign and very close in magnitude to ours based on dipole–dipole interaction energies alone (cf. eq 2). Furthermore, the sign and intensity patterns of the calculated spectra using the two models agree well. The calculated results predict a conservative couplet for the α-helical conformation, yet the observed results reveal the integrated negative peak is larger than the positive one by a factor of 1.2. (In the spectra of the "random coil" conformation, vide infra, the negative lobe is larger by a factor of 1.5.) Thus, it is clear that exciton interactions cannot explain the observed optical activity completely and other factors contribute to the observed VCD. We have shown before that an uncoupled amide I′ vibration in dipeptides composed of L-amino acids exhibits negative VCD intensity (Roberts et al., 1988). Thus, the negative bias of the observed VCD spectra in PLT could result from optical activity induced in the C=O chromophore by the chirality of the amino acid residues, or from other factors such as charge flow between oscillators.

Inspection of the eigenvectors reveals that nearly all negative VCD intensity is due to the component polarized parallel to the helix axis, as predicted by Snir. However, the strong infrared absorption intensity calculated for this peak appears at higher frequency than the zero crossing of the VCD spectrum, whereas the observed IR spectrum has its absorption maximum under the positive part of the VCD couplet. This is a quite serious discrepancy, which was correctly pointed out by one referee of this paper. Within the exciton formalism, there is no explanation for this discrepancy, but possible causes, involving vibrational interactions, will be discussed below.

We used a much shorter peptide sequence (an octamer) for our computations, whereas Schellman used a 36-mer. We find that the spectral features produced with an octamer are virtually indistinguishable from those of a longer polymer. Indeed, when the polymer length exceeds about 12, the spectral amplitudes appear to be slightly decreasing, due to cancelation of many positive and negative contributions. This observation is not true for the rotational strengths R_k, when no band shape effects are taken into account. The values of the dominant terms R_k, in fact, approach a value nearly independent of the chain length, which is given by the coupling interaction. Our computed results are about a factor of 2 weaker than the observed ones, independent of the peptide length and band shape parameters.

The computed features shown in Figure 2 are obtained, as previously in the case of computed DNA VCD, with no adjustable parameters. To facilitate a comparison with the work of Schellman and co-workers, we utilized in these computations 100% Gaussian band envelopes, although we have found previously that 50:50 Gaussian/Lorentzian mixtures give slightly better fits to the observed spectra. As mentioned before, the dipole strength of the amide I transition and its unperturbed vibrational frequency were taken from our previous peptide studies (Lee et al., 1989) and agree well with Schellman's data. These parameters were not allowed to vary to reproduce the α-helical spectral features.

The calculated VCD spectrum is nearly exactly a factor of 2 smaller than the observed one, whereas the calculated absorption spectrum is slightly larger than the experimental data. In addition, the calculated infrared absorption spectrum is significantly narrower than the observed one. We believe that these three discrepancies all arise from the same problem. In our calculations, only dipole–dipole coupling between the amide I vibrations was considered. In reality, one expects vibrational coupling (through the vibrational force field) to contribute significantly to the interaction between the dipoles, and, thus, increase the splitting between the exciton components. This, in fact, will reduce the cancelation of positive and negative exciton components, increasing the magnitude of the VCD spectra and the half-width of the absorption spectra. It also could effect the computed peak positions. The same arguments had to be made before when the VCD spectra of $(L\text{-Ala})_3$ were fitted with computational data (Lee et al., 1989). In this case, the computed splitting between the coupled oscillator components was also much smaller than the observed splitting, which reduced the computed VCD intensities.

We have initiated calculations which take into account the force field effects on the computed VCD spectra. This procedure involves calculating the normal modes of the peptide backbone explicitly, in a fashion similar to the calculations reported by Moore and Krimm (1976). The potential energy matrix is then augmented by the dipole–dipole interaction energies described in eq 2. The aim of these calculations is to use the complete vibrational eigenvectors to compute the VCD intensities according to eq 1. This procedure, in principle, should account for the observed differences in VCD band shapes for α-helical peptides between amide I and amide I′ vibrations, i.e., upon deuteriation of the amide proton. These calculations are well underway, and preliminary results indicate that the splitting between the exciton components is, indeed, significantly larger when the vibrational coupling is taken into account. Furthermore, a better understanding of the splitting and ordering of the exciton components is expected to emerge. An improper ordering of the eigenvalues and eigenvectors in the pure exciton calculations could, conceivably, be responsible for the improper position of the absorbance maximum relative to the VCD zero-crossing in the calculated spectra presented. However, these calculations are significantly more complicated, and depend on many more parameters than the simple vibrational exciton calculations presented so far. Thus, they will not be useful for some time until all parameters are optimized. In the meantime, the vibrational exciton model, which has severe limitations, offers the only practical method of computing VCD intensities for a molecule of this magnitude. In light of the shortcomings of the ECO model, the agreement between observed and calculated VCD spectra for the α-helical amide I region (cf. Figure 2) is excellent.

The computation presented so far established the limits of reliability of the computational procedures for a well-established peptide conformation. Next, computed VCD results for possible left-handed structures will be presented. Previously, CD and vibrational arguments have been presented (Tiffany & Krimm, 1968; Sengupta & Krimm, 1987) suggesting that the "random coil" conformation might be an extended left-handed helical structure. Thus, we calculated VCD intensities for a number of left-handed structures in order to establish whether or not these structures exhibit computed VCD features similar to the ones observed. However, we did not attempt to analytically fit computed vs observed spectra by varying the angles ϕ and ψ systematically, since such a fitting procedure is extremely complicated, given the varying sign and magnitude of the exciton splitting, intensity cancelations, etc.

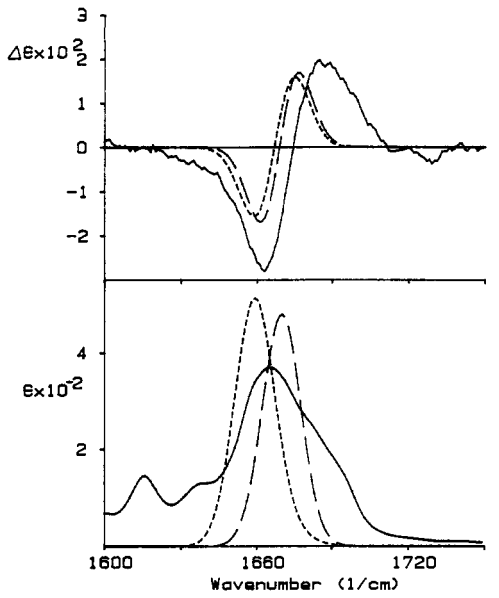

FIGURE 3: Observed (solid traces) and computed (dashed traces) spectra of "random coil" poly(L-tyrosine). Experimental conditions: same as in Figure 1. Computational conditions: (short dashes) octamer, $\phi = 60°$, $\psi = 30°$; (long dashes) octamer, $\phi = -110°$, $\psi = 120°$.

Instead, we computed VCD intensities for a number of conformers in the vicinity of energy minima in the Ramachandran plot. The region with $\phi = -110°$ and $\psi = 120°$, close to the pleated-sheet conformation (Creighton, 1984), produced structures with good agreement with the observed spectra. In addition, the region around the left-handed α-helix (60°, 50°) yielded similar agreement. In both cases, it was found that the conformations with more residues per turn (for example, with ϕ and ψ values of 60° and 75°, respectively) reproduced the spectra less satisfactorily than more extended structures with less than three residues per turn.

The criteria used to select the best fit were as follows. We searched for a conformation where the computed spectrum was about 50–70% of the observed ones, since one may assume that the vibrational coupling is too low for the "random coil" conformer as well, and since the α-helical structure yielded too low computed spectra by a similar amount. In addition, the crossover point in the VCD spectra (observed at 1661 cm^{-1} for α-helical and 1674 cm^{-1} for the "random coil" conformation) was used as a criterion. Finally, the overall intensity pattern and band shapes were required to be as close as possible to the observed ones.

The computed VCD spectra of two conformers fulfilling these requirements are shown in Figure 3. One of these structures has the conformational angles $\phi = 60°$ and $\psi = 30°$. This conformer falls at the very edge of a conformational energy minimum in the Ramachandran plot and has a ϕ angle similar to that of the left-handed α helix, but is more extended. This structure is stabilized by internal hydrogen bonds similar to those found in a right-handed α-helix. Calculated VCD spectra for a number of structures in the vicinity of the left-handed α-helix were very similar to each other, and increased in magnitude as the number of residues per turn increased.

The other structure, which fits the observed spectra well, is qualitatively similar to the extended, left-handed structure with 2.5 residues per turn suggested by Krimm (Sengupta & Krimm, 1987) for the "random coil" conformation. Our calculations suggest a structure with ϕ and ψ angles of $-110°$ and 120°, respectively. This structure is very close to the dividing boundary between left- and right-handed structures in the Ramachandran map [see, for example, Dickerson and Geis (1969)]. Indeed, changing the conformational angles by a few degrees switches the sign patterns of the computed VCD features. This structure does not have intramolecular hydrogen bonds, and is even further extended than the extended helix (EH) postulated by Krimm.

The fit between the VCD spectra computed for these two conformers and the observed spectra is about equally good. The extended structure has a zero crossing somewhat closer to the observed one. The rotational strengths calculated for the extended structure are much larger (by a factor of 3) than those calculated for the left-handed α-helix; however, the splitting is much smaller in the extended structure, and cancelation reduces the intensities to levels similar to those calculated for the left-handed α-helix.

On the basis of the VCD data alone, we cannot decide between the two computed structures. However, there are a few facts that make us believe that the extended structure is more likely to describe the "random coil" conformation best. First, prior CD and vibrational studies by Krimm and his co-workers favor the extended form. Second, the left-handed α-helix has a hydrogen-bonding pattern similar to that of the right-handed α-helix; thus, it is not intuitively clear why acidification of a DMSO solution should favor one conformer over the other. Finally, a left-handed α-helix has not been found via crystallographic techniques, whereas the extended left-handed helical form falls into a broad region of many established structural motifs in peptides.

Conclusions

We have demonstrated that the ECO formalism may be used to compute VCD features of homooligopeptides in the amide I region. Although a solution structure of the peptide conformation generally referred to as the "random coil" cannot yet be derived from VCD data unambiguously, we have shown that several left-handed helices exhibit VCD spectra similar to the one observed. This result suggests that the "random coil" conformation has high order on the VCD interaction length, which may be judged from the coupling energies to be at least five residues. Among two conformers which fit the observed VCD features, we favor the one which is similar to the extended helix described by Krimm and co-workers (Sengupta & Krimm, 1987).

In the stage of the final revision of this paper, the authors received a copy of a manuscript from Prof. Keiderling (Dukor & Keiderling, 1991) which reassesses the "random coil" peptide conformation via an analysis of VCD, IR, and CD spectra of proline oligopeptides. This paper, which includes a critical review of the pertinent literature, reaches nearly identical conclusions.

Acknowledgments

We thank Prof. T. A. Keiderling (University of Illinois at Chicago) for making available a preprint of the work on proline oligopeptides.

Registry No. PLT, 25667-16-7.

References

Creighton, T. E. (1984) *Proteins: Structures and Molecular Principles*, W. H. Freeman and Co., New York.

Deutsche, C. W., & Moscowitz, A. (1968) *J. Chem. Phys. 49*, 3257.

Deutsche, C. W., & Moscowitz, A. (1970) *J. Chem. Phys. 53*, 2630.

Dickerson, R. F., & Geis, I. (1969) *The Structure and Action of Proteins*, Harper & Row, Publishers, New York.

Diem, M., Roberts, G. M., Lee, O., & Barlow, A. (1988) *Appl. Spectrosc. 42*, 20.
Dukor, R. K., & Keiderling, T. A. (1991) *Biopolymers* (in press).
Greenfield, N. J., & Fasman, G. D. (1969) *Biochemistry 8*, 4108.
Gulotta, M., Goss, D. J., & Diem, M. (1989) *Biopolymers 28*, 2047.
Holzwarth, G., & Doty, P. (1965) *J. Am. Chem. Soc. 87*, 218.
Keiderling, T. A. (1990) in *Practical Fourier Transform Infrared Spectroscopy*, pp 203-283, Academic Press, New York.
Lee, O., Roberts, G. M., & Diem, M. (1989) *Biopolymers, 29*, 1759.
Lipp, E. D., & Nafie, L. A. (1985) *Biopolymers 24*, 799.
Miyazawa, T., & Blout, E. R. (1961) *J. Am. Chem. Soc. 83*, 712.
Moore, W. H., & Krimm, S. (1976) *Biopolymers 15*, 2439.
Paterlini, G. M., Freedman, T. B., & Nafie, L. A. (1986) *Biopolymers 25*, 1751.
Roberts, G. M., Lee, O., Calienni, J., & Diem, M. (1988) *J. Am. Chem. Soc. 110*, 1749.
Schellman, J. (1973) *J. Chem. Phys. 58*, 2882.
Schellman, J., & Becktel, W. J. (1983) *Biopolymers 22*, 171.
Schulz, G. E., & Schirmer, R. H. (1979) *Principles of Protein Structure* (Cantor, C. R., Ed.) Springer-Verlag, New York.
Sengupta, P. K., & Krimm, S. (1987) *Biopolymers 26*, S99.
Snir, J., Frankel, R. A., & Schellman, J. A. (1975) *Biopolymers 14*, 173.
Still, C. (1989) MacroModel Version 2.5, Columbia University, New York.
Tiffany, M. L., & Krimm, S. (1968) *Biopolymers 6*, 1379.
Tinoco, I. (1963) *Radiat. Res. 20*, 133.
Wen, K. J., & Woody, R. W. (1975) *Biopolymers 14*, 1827.
Yasui, S. C., & Keiderling, T. A. (1986a) *Biopolymers 25*, 5.
Yasui, S. C., & Keiderling, T. A. (1986b) *J. Am. Chem. Soc. 108*, 5576.
Zhong, W., Gulotta, M., Goss, D. J., & Diem, M. (1990) *Biochemistry 29*, 7485.

High-Resolution Solid State ^{13}C NMR of Bacteriorhodopsin: Characterization of [4-^{13}C]Asp Resonances†

Günther Metz,‡ Friedrich Siebert,*,‡,§ and Martin Engelhard‖

Institut für Biophysik und Strahlenbiologie der Universität Albertstrasse 23, D-78 Freiburg, FRG, Max-Planck-Institut für Biophysik, Kennedy-Allee 70, D-6 Frankfurt, FRG, and Max-Planck-Institut für Ernährungsphysiologie, Rheinlanddamm 201, D-46 Dortmund, FRG

Received March 5, 1991; Revised Manuscript Received October 1, 1991

ABSTRACT: Solid state ^{13}C nuclear magnetic resonance measurements of bacteriorhodopsin labeled with [4-^{13}C]Asp show that resonances of single amino acids can be resolved. In order to assign and characterize the resonances of specific Asp residues, three different approaches were used. (1) Determination of the chemical shift anisotropy from side-band intensities provides information about the protonation state of Asp residues. (2) Relaxation studies and T_1 filtering allow one to discriminate between resonances with different mobility. (3) A comparison of the spectra of light- and dark-adapted bacteriorhodopsin provides evidence for resonances from aspartic acid residues in close neighborhood of the chromophore. In agreement with other investigations, four resonances are assigned to internal residues. Two of them are protonated in the ground state up to pH 10 (Asp_{96} and Asp_{115}). All other detected resonances, including Asp_{85} and Asp_{212}, are due to deprotonated aspartic acid. Two lines due to the two internal deprotonated groups change upon dark and light adaptation, whereas the protonated Asp residues are unaffected.

The retinal protein bacteriorhodopsin (BR),[1] found in the purple membrane of *Halobacterium halobium*, acts as a light-driven proton pump [for a review, see Stoeckenius and Bogomolni (1982)]. Recently, a model for the structure of BR has been obtained from high-resolution electron cryomicroscopy (Henderson et al., 1990) showing the atoms of the membrane-embedded part of the protein. The retinal chromophore is bound to Lys_{216} via a protonated Schiff base, and its reversible photoisomerization initiates the BR photocycle. Several intermediates K, L, M, N, and O can be distinguished by their visual absorbance (Lozier et al., 1975; Kouyama et al., 1988). Detailed models for the pumping mechanism of BR, based on different experimental investigations, have been proposed (Engelhard et al., 1985; Braiman et al., 1988; Fodor et al., 1988; Khorana, 1988; Henderson et al., 1990).

The deprotonation of the Schiff base in M is an essential step for the pumping activity (Longstaff & Rando, 1987). The observation of protonation changes of carboxyl groups during the BR photocycle suggested an important role of Asp/Glu residues in proton transport (Siebert et al., 1982; Rothschild et al., 1981). Numerous infrared studies, including the use

† This work was supported by the Deutsche Forschungsgemeinschaft SFB 60-G9.
* To whom correspondence should be addressed.
‡ Institut für Biophysik und Strahlenbiologie der Universität.
§ Max-Planck-Institut für Biophysik.
‖ Max-Planck-Institut für Ernährungsphysiologie.

[1] Abbreviations: BR, bacteriorhodopsin; CSA, chemical shift anisotropy; BR_{la}, light-adapted bacteriorhodopsin; BR_{da}, dark-adapted bacteriorhodopsin; CP, cross polarization; NMR, nuclear magnetic resonance; MAS, magic angle spinning; FTIR, Fourier transform infrared.

0006-2960/92/0431-455$03.00/0